Optimal Search Strategies for Pollutant Source Localization*

Behzad Bayat[1], Naveena Crasta[2], Howard Li[3] and Auke Ijspeert[1]

***Abstract*— This paper is aimed at developing optimal motion planning for a single autonomous surface vehicle (ASV) equipped with an on-board pollutant sensor that will maximize the sensor-related information available for source seeking. The ASV uses a nonlinear diffusion model of the pollutant source to estimate the intensity/level of the pollution at the present ASV location. The rate of detection of particles depends on the relative distance between the ASV and the source. First, we use a probabilistic map of the source location built through the sensor information for a dynamic motion planning of source seeking based on an entropy reduction formulation, where an appropriately defined Fisher information matrix (FIM) is used for entropy reduction or information gain. We derive the FIM for the set-up and investigate optimal trajectories. Next, we present an online nonlinear Monte Carlo algorithm that uses the obtained sensor information about pollutant at different vehicle locations to update a probabilistic uncertainty map of pollutant source location. As the mission unfolds the ASV motion is computed by considering a moving-horizon interval of decision, which will allow for the inclusion of new information available for optimal motion planning. The proposed motion planning approach is extended to take into account external disturbances and it is able to minimize the uncertainty in the pollutant source. Finally, we provide two case studies to demonstrate efficacy of the proposed motion planning algorithm.**

I. INTRODUCTION

In recent years, the problem of source localization has been studied in wide variety of applications. Source seeking involves driving single/multiple vehicles that provide a search platform to take measurements of the emitted quantity, towards the source, with limited or no position information. The applications are numerous such as ocean sampling, explosive detection, sensing hazardous chemicals and pollution sensing, to name a few among others.

Methods in the literature use either the gradient-based search [1], coverage search [2] for unknown pollutant source seeking, building of flow field maps [3], and bio-inspired search methods [4]. Some of the earlier methods, such as [5], use tracks or spirals to reduce the localization uncertainty for unknown source seeking. In a turbulent medium like air or water, turbulent flow causes random and disconnected patches which makes the gradient of information uncertain to be used for guidance in source seeking. A more recent method, "*Infotaxis*", introduced by [6] is proposed as a search strategy based on theoretical information principles to maximize the entropy reduction. Several studies exploited this gradient-free idea, such as the most recent one in [7] and references therein, for many different search scenarios.

In this work, optimal search strategies are investigated for pollutant source localization using an autonomous surface vehicle (ASV). Since the ASV location is known, we can predict the mean concentration of pollutants using the relative distance from the estimated pollutant source location. The actual pollutant measurement can be used to impart a proper motion on the ASV in order to reduce the mean concentration uncertainty and the pollutant source location uncertainty. We maintain the probability of pollutant source location in the workspace through the pollutant diffusion model and the measurement uncertainty. This approach has the distinct advantage that we can now use the pollutant source location uncertainty information to plan optimal paths that adaptively account for the pollutant source location uncertainty. We propose that an entropy reduction approach is appropriate for planning these paths. The probabilistic search method is particularly suited to the unknown source seeking mission. This paper proposes an approach for auto-navigation of Envirobot [8], towards the goal of localizing and approaching pollutant sources at water surface, where the ASV must guide its movements and sampling on the basis of the sensory input. This approach has been used in variety of problem and resulted in interesting theoretical results but experimental realization were very limited. Recently, in [9] authors proposed a Fisher based integrated motion planning, control and estimation algorithm and successfully tested the algorithm in field experiment.

To summarize, the contributions of the presented work are twofold.

- Based on a probabilistic sensor model and kinematic model of the ASV, Fisher information matrix (FIM), which is directly related to the minimum covariance achievable with any unbiased estimator, is analytically derived.
- An optimal motion planning algorithm based on the probabilistic representation is proposed that adaptively accounts for pollutant source location uncertainty and pollutant emission rate uncertainty. Source seeking is posed as an entropy reduction problem using the FIM and optimal paths are planned to satisfy the objective function.

The organization of the paper is as follows. The problem is formulated in probabilistic terms in Section II. Based on

*This work is supported in part by Envirobot, a project of the Swiss NanoTera program, Natural Sciences and Engineering Research Council of Canada (NSERC), and EC CADDY (FP7-ICT-2013, Grant Agreement No. 611373).

[1]Behzad Bayat and Auke Ijspeert are with BioRobotics Laboratory, Ecole Polytechnique Fédérale de Lausanne (EPFL), Switzerland, {behzad.bayat,auke.ijspeert}@epfl.ch

[2]Naveena Crasta is with Institute for Systems and Robotics (ISR), Instituto Superior Técnico (IST), University of Lisbon, Portugal, ncrasta@isr.ist.utl.pt

[3]Howard Li is with COBRA, Department of Electrical and Computer Engineering, University of New Brunswick, Fredericton, NB E3B 5A3, Canada, howard@unb.ca

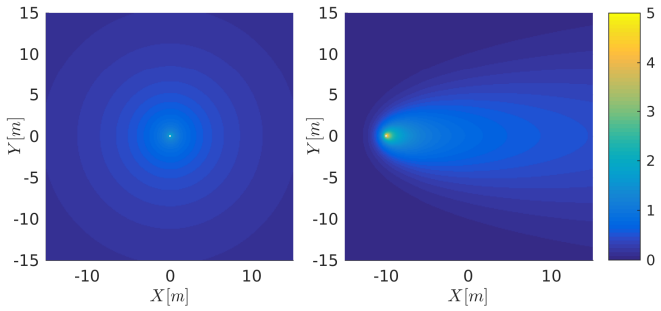

Fig. 1: Expected rate of detected particles for a pollution source: (left) $\boldsymbol{v}_c = \mathbf{0}$ and (right) $\boldsymbol{v}_c = [1, 0]'$.

the probabilistic formulation, the information-based optimal search strategies are proposed in Section III for pollutant source seeking; and the Monte Carlo method is developed to localize the unknown pollutant source. Simulation results are presented in Section IV and finally the paper concludes in Section V with future directions.

II. Problem Formulation

In many of the environmental applications, the detection of chemicals in water is a very critical issue and ASVs are providing sensor/search platforms that offer durability and great area coverage, while keeping the risk involved to a minimum. The experimental set-up considered in this article consists of a search platform moving in the presence of unknown disturbances and that is equipped with an on-board pollutant sensor suite, which uses the nonlinear diffusion model of the pollutant to estimate the intensity/level of the pollutant at the present ASV location.

Let $\boldsymbol{s} := [s_x, s_y]' \in \mathbb{R}^2$ and $\boldsymbol{r} := [x, y]' \in \mathbb{R}^2$ denote the inertial position of the stationary pollution source (modeled as a point source) and the instantaneous inertial position of a search platform, respectively, and we assume that the pollutant is emitting particles at the constant unknown emission rate of $Q_0 > 0$. We adopt the model for the turbulent transport of particles through the medium from [6], [7]. The average lifetime of particles propagating with the isotropic diffusivity $D[\mathrm{m/s^2}]$ is $\tau[\mathrm{s}]$ and the particles are subjected to external disturbances such as wind/current with the measured speed of advection $\boldsymbol{v}_c = [v_{cx}, v_{cy}]' \in \mathbb{R}^2$. As the ASV moves, the spherical shaped on-board sensor, which is of size $a[\mathrm{m}]$, experiences a series of encounters with emitted particles at the rate

$$R(\boldsymbol{r}, \boldsymbol{s}) = \frac{Q_0}{\ln(\lambda/a)} \exp\left[\frac{\boldsymbol{v}_c'(\boldsymbol{r}-\boldsymbol{s})}{2D}\right] K_0\left(\frac{\|\boldsymbol{r}-\boldsymbol{s}\|}{\lambda}\right), \quad (1)$$

where $\|\cdot\|$ is the Euclidean norm, $K_0(\cdot)$ is the modified zero order Bessel function of second kind [10, p. 232] and

$$\lambda \triangleq \sqrt{\left(1 + \frac{\|\boldsymbol{v}_c\|^2 \tau}{4D}\right)^{-1} D\tau}. \quad (2)$$

In (1), by $R(\boldsymbol{r}, \boldsymbol{s})$ we mean the rate of emitted particles at the present location $\boldsymbol{r}$ given the source located at $\boldsymbol{s}$, and for the sake of simplicity we suppress its dependency on the various variables.

Fig. 1 shows expected rate of detected particles for a pollution source with parameters, $Q_0 = 1$, $\tau = 250$, $D = 1$, and $a = 1$ for the case $\boldsymbol{v}_c = [1, 0]'$ and $\boldsymbol{v}_c = \mathbf{0}'$. The particles tend to move in the direction of the current, which results in elliptical shaped contours as shown in the right figure, while they becomes circular in the absence of currents as depicted in the left figure.

The process of sensor encounters with emitted particles is stochastic and can be modeled using the Poisson distribution [6], [7]. The probability that the sensor at location $\boldsymbol{r}$ encounters $z(\boldsymbol{r}) \in \mathbb{Z}^+$ particles during a time interval of $\Delta t[\mathrm{s}]$ is

$$p(z(\boldsymbol{r}), \mu) = \mu^{z(\boldsymbol{r})} \exp[-\mu]/z(\boldsymbol{r})!, \quad (3)$$

where $\mu \triangleq R(\boldsymbol{r}, \boldsymbol{s})\Delta t$ is the mean concentration. Assuming that a, τ, D, $\boldsymbol{v}_c$, and Q_0 are known, (3) represents the full specification of the *likelihood function* of $\boldsymbol{s}$, given a measurement $z(\boldsymbol{r})$ taken at location $\boldsymbol{r}$, and we denote this likelihood function by $p(z(\boldsymbol{r})|\boldsymbol{s})$.

Let $\boldsymbol{r}_0 := [x_0, y_0]' \in \mathbb{R}^2$ be the initial position of the ASV at the initial time t_0. The discretized kinematics of the ASV is given by

$$\boldsymbol{r}_{i+1} = \boldsymbol{r}_i + \left(v\begin{bmatrix}\cos\psi_i \\ \sin\psi_i\end{bmatrix} + \boldsymbol{v}_c\right)(t_{i+1} - t_i),\ i \in \{0, 1, .., m-2\}, \quad (4)$$

where $m \in \mathbb{N}$ is the number of samples, $v > 0$ is the constant body-speed, $\psi_i \in (-\pi, \pi]$ is the piecewise constant course angle and $\boldsymbol{v}_c \in \mathbb{R}^2$ is constant current vector. Clearly, for m samples, from (4) it is evident that we need $m-1$ piecewise constant course angles. Given the sensor model (1), the probability density function of the measurements (3), and the ASV's model (4), we are interested in the following question:

> *"Given a temporal window and the initial ASV location, what are the best sequences of actions for the ASV that can maximize the sensor-related information about the source location?"*

To make this more precise, we use FIM as a measure of information as it is directly related to the minimum covariance achievable with any unbiased estimator. This result is also known as Crámer-Rao Lower Bound [11, Sec. 2.7]. In the following section we calculate the FIM related to this problem for a hypothetical pollutant source which would help us in finding the best possible action for maximizing information about the pollutant source location.

III. Methodology

Fig. 2 shows block diagram of the overall approach to the problem. The ASV is modeled by the kinematics with course angle as input and inertial position as the state vector. In addition, the ASV is equipped with GPS and hence its position is known accurately. Depending on the ASV position, the on-board sensor provides information about source location through detection of particles emitted from the source. A *particle filter* (PF) uses the measurements to generate an estimate of the source location and emission rate of pollutant at source location through a multiple hypothesis set-up. The *optimal trajectory planner*, then uses these hypotheses and

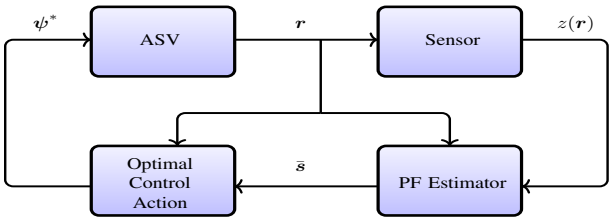

Fig. 2: Block diagram of the overall approach to the source seeking problem.

computes an optimal control sequence (vector of course angles) for each hypothesis to maximize information about the source location. The optimal control sequence with most collective weighted votes from hypotheses is selected as applied control action to the ASV. As a result, maximizing the information about the source location drives the ASV towards the source, which will be elaborated in Sec. III-A.

In what follows, we describe optimal planner and estimator blocks in detail.

A. Optimal Control Action

As our task demands investigation of ASV trajectories that will maximize the sensor information available for source seeking, we use a scalar function of an appropriately defined FIM as the performance index for the controller. The optimal control action uses the ASV position and the estimated source location from the PF estimator and provides the optimal course angle. To fix the ideas, we first derive the FIM associated with location of the source as the paramter, and next we provide the optimal control problem formulation.

1) Derivation of FIM: To derive FIM about the unknown parameter $\boldsymbol{s}$, consider a finite sequence of data points $\{(\boldsymbol{r}_i, z_i(\boldsymbol{r}_i))\}_{i=0}^{m-1}$, $m \geq 2$, where for each $i \in \{0, 1, \ldots, m-1\}$, z_i denotes the measurement at the ASV location $\boldsymbol{r}_i$ and time instant t_i, as shown in Fig. 3. For each $i \in \{1, \ldots, m-1\}$, observe that $\boldsymbol{r}_i$ depends on the action ψ_{i-1} as evident from (4). Denote $\boldsymbol{\psi} \triangleq (\psi_0, \ldots, \psi_{m-2})$, $X \triangleq (\boldsymbol{r}_0, \boldsymbol{r}_1, ..., \boldsymbol{r}_{m-1})$, and $\boldsymbol{z} \triangleq [z_0, z_1, ..., z_{m-1}]'$, and we let $FIM_{\boldsymbol{\psi}}(\boldsymbol{s}) \in \mathbb{R}^{2\times 2}$ denote the FIM. Under certain regularity conditions [11, Sec. 2.7], $FIM_{\boldsymbol{\psi}}(\boldsymbol{s})$ is given by

$$FIM_{\boldsymbol{\psi}}(\boldsymbol{s}) \triangleq \mathbb{E}\left\{ [\nabla_{\boldsymbol{s}} \ln p(\boldsymbol{z}(X)|\boldsymbol{s})] [\nabla_{\boldsymbol{s}} \ln p(\boldsymbol{z}(X)|\boldsymbol{s})]' \right\}, \quad (5)$$

where $p(\boldsymbol{z}(X)|\boldsymbol{s})$ is the likelihood function of the measurement vector $\boldsymbol{z} \in \mathbb{R}^m$ with respect to the parameter $\boldsymbol{s}$, and $\mathbb{E}$ and ∇ are expectation and gradient operators, respectively.

From (1) notice that one of the strategies is to sample in the close vicinity of the source because the expected rate of detecting pollutant particles gets higher as the ASV gets closer to the source. However, given the speed limit and restricted maneuverability of the ASV coupled with limitation on measurement sampling frequency, this strategy may not be the best when the starting position of the ASV is considerably far away from the source. Further, the situation is complicated by the presence of currents also as the strategy significantly depends on the direction and magnitude of the current. Using (3) in (5) with some algebraic manipulations,

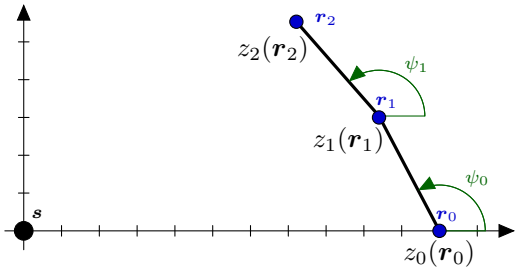

Fig. 3: A trajectory of the ASV starting from a distance $\|\boldsymbol{r}_0 - \boldsymbol{s}\|$ with $\boldsymbol{v}_c = 0$, and taking measurements z_i, $i = 0, 1, 2$, at the instant t_i, while the ASV is at $\boldsymbol{r}_i$ under the action of piecewise constant course angle.

we get

$$FIM_{\boldsymbol{\psi}}(\boldsymbol{s}) = \frac{Q_0 \Delta t}{4\lambda^2 D^2 \ln\left(\frac{\lambda}{a}\right)} \sum_{i=0}^{m-1} \exp\left[\frac{\boldsymbol{v}_c' \boldsymbol{q}_i}{2D}\right] \left(\frac{\boldsymbol{p}_i \boldsymbol{p}_i'}{K_{0,i}}\right), \quad (6)$$

where, for each $i \in \{0, \ldots, m-1\}$, $\boldsymbol{p}_i \triangleq \lambda K_{0,i} \boldsymbol{v}_c - 2DK_{1,i}\boldsymbol{q}_i/\|\boldsymbol{q}_i\|$, $\boldsymbol{q}_i \triangleq \boldsymbol{r}_i - \boldsymbol{s}$, $K_1(\cdot)$ is the modified zero order Bessel function of second kind, $K_{0,i} \triangleq K_0(\|\boldsymbol{q}_i\|/\lambda)$, and $K_{1,i} \triangleq K_1(\|\boldsymbol{q}_i\|/\lambda)$. Now, in the absence of current, i.e., $\boldsymbol{v}_c = \boldsymbol{0}$, (6) becomes

$$FIM_{\boldsymbol{\psi}}(\boldsymbol{s}) = \frac{Q_0 \Delta t}{\lambda^2 \ln\left(\frac{\lambda}{a}\right)} \sum_{i=0}^{m-1} \left(\frac{K_{1,i}^2}{K_{0,i}}\right) \left(\frac{\boldsymbol{q}_i \boldsymbol{q}_i'}{\boldsymbol{q}_i' \boldsymbol{q}_i}\right). \quad (7)$$

Notice that in this particular case, (7) reveals that the FIM is a weighted sum of outer product of the normalized relative position vector, where the weighting function $f(\boldsymbol{r}_i, \boldsymbol{s}) \triangleq K_{1,i}^2/K_{0,i}$ only depends on the relative distance $\|\boldsymbol{q}_i\|$. Further, the right-hand side of (7) has two terms: i) a scalar function $f(\cdot)$ and ii) a normalized outer product. The first term $f(\cdot)$ has the property that it grows in magnitude as the ASV gets closer to the source, while the second term alone has a striking resemblance with the single-beacon navigation problem in the underwater robotics field [12] and as it is shown in [13], a circular motion around the source would improve the information about the source location, meaning richer FIM. These two observations leads us to conjecture that a possible expected optimal trajectory is an inward spiral motion towards the source.

2) Optimal Control Problem Formulation: In order to maximize information about the parameter $\boldsymbol{s}$, we consider the scalar cost function

$$J(\boldsymbol{\psi}) \triangleq \ln |FIM_{\boldsymbol{\psi}}(\boldsymbol{s})|, \quad (8)$$

where $|\cdot|$ denotes the determinant of a matrix.

With this, we are now equipped to define the optimal control problem of finding a sequence of actions $\boldsymbol{\psi}$ that maximizes the cost function (8), i.e., information about the parameter $\boldsymbol{s}$. Mathematically this leads to the following optimal control problem:

$$\boldsymbol{\psi}^* = \underset{\text{subject to:}(4), \boldsymbol{r}_0 \in \mathbb{R}^2}{\arg\max} \; J(\boldsymbol{\psi}). \quad (9)$$

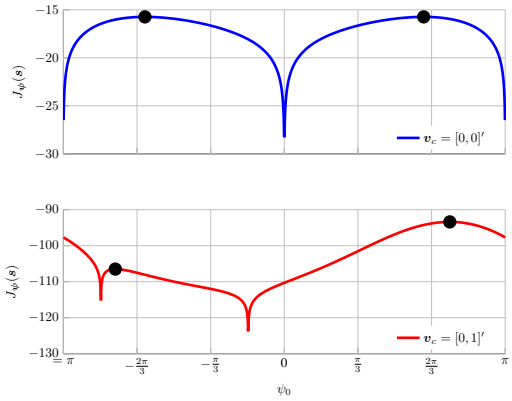

Fig. 4: Plot of $J(\boldsymbol{\psi})$ as a function of $\psi_0 \in (-\pi, \pi]$.

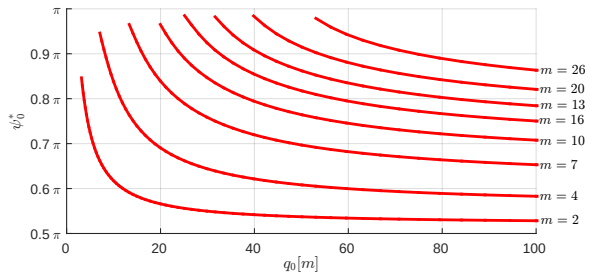

Fig. 5: Solution of optimization problem (9) as a function of q_0 for various values of m.

In order to give a glimpse of the behavior of the cost function, we present the numerical evaluation of $J(\boldsymbol{\psi})$ for $\boldsymbol{v}_c = \mathbf{0}$ and $\boldsymbol{v}_c = [1, 0]'$. Fig. 4 shows the plot of $J(\boldsymbol{\psi})$ for the ASV speed $v = 2[\mathrm{m/s}]$, sampling time 1[s], relative initial position of ASV $\boldsymbol{q}_0 = [100, 0]'[\mathrm{m}]$, and $m = 5$ samples. Sensor and pollution source parameters are set to the ones presented in Fig. 1. In this case, $J(\cdot)$ is a function of single variable ψ_0. Note that for $\boldsymbol{v}_c = \mathbf{0}$, the cost function has two isolated global maxima where one is in $(\pi/2, \pi]$ and the other in $[-\pi, -\pi/2)$. On the other hand, for $\boldsymbol{v}_c = [1, 0]'$, one becomes absolute maximum, while the other one turns into a local maximum.

In what follows, we investigate the optimal trajectories that maximizes the FIM for the two cases, namely, i) without currents and ii) with currents. To begin with, we first analyze the simple situation where the current is zero.

Case I (without current): Let $q_i \triangleq \|\boldsymbol{r}_i - \boldsymbol{s}\|$, $i \in \{0, 1, \ldots, m-1\}$, and $h \triangleq (t_{j+1} - t_j)$, $j \in \{0, 1, \ldots, m-2\}$ as we assume uniform sampling. Since the term $\frac{Q_0 \Delta t}{\lambda^2 \ln\left(\frac{\Delta}{a}\right)}$ is a constant and intrinsic property of the sensor and the source, it will not change the optimal solution $\boldsymbol{\psi}^*$ based on the cost function defined in (8). Thus, it will not be shown in the computation of the determinant of FIM.

With this, in this particular case we get

$$|FIM_{\boldsymbol{\psi}}(\boldsymbol{s})| = (vh)^2 \sum_{i=1}^{m-1} \frac{f(q_i)}{q_i^2} \sum_{j=0}^{i-1} \frac{f(q_j)}{q_j^2} \left(vh \sum_{k=0}^{j-1} \sum_{l=j}^{i-1} \sin(\psi_k - \psi_l) - q_0 \sum_{k=j}^{i-1} \sin(\psi_k)\right)^2. \quad (10)$$

Notice that in this case, the cost function $J(\cdot)$ is a function of $m-1$ variables. In particular, if the ASV moves on a straight line, that is, $\psi_i \triangleq \psi_0 \in (-\pi, \pi]$ for all $i \in \{0, \ldots, m-1\}$, then (10) reduces to

$$|FIM_{\boldsymbol{\psi}}(\boldsymbol{s})| = (vhq_0 \sin\psi_0)^2 \sum_{i=1}^{m-1} \frac{f(q_i)}{q_i^2} \sum_{j=0}^{i-1} \frac{f(q_j)(i-j+1)^2}{q_j^2}, \quad (11)$$

thereby reducing $J(\cdot)$ to a function of single-variable. To see the optimal course angle for this particular case, without loss of generality and due to symmetry (see Fig. 1, right) of the diffusion process model (1), we assume that the ASV starts from $\boldsymbol{q}_0 = [q_0, 0]'$. The sensor takes m samples that includes the initial and the terminal point. Fig. 5 shows the solution of optimization problem (9) as a function of initial distance to the source q_0 for different number of samples m, ASV speed $v = 2[\mathrm{m/s}]$, sampling time $h = 1[\mathrm{s}]$, and sensor and pollution source parameters are set to the ones presented in Fig. 1. From Fig. 5 we can conclude that increasing the look ahead distance, which is the same as increasing number of samples in FIM, results in the optimal course angle ψ_0^* being closer to π. Fig. 6 shows the numerical result of this search strategy for selected number of samples m and corresponding evolution of FIM versus the distance covered by the ASV. Notice that, as we increase m, the spiral motion becomes tighter. Since the final goal is to approach pollution source, one strategy is to start with larger look ahead distance and decrease it as the ASV gets closer to the source.

So far, using (11) we looked at optimal trajectories as a consequence of considering constant course angle during the look ahead time horizon. Now consider the more general case given by (10). Recall that now $J(\cdot)$ is a function of $m-1$ variables. Nevertheless, the resulting cost function has two isolated maxima, where one lies in $(\pi/2, \pi]^{m-1}$ and the other in $[-\pi, -\pi/2)^{m-1}$. Fig. 7 presents the optimization results for different number of samples m, ASV speed $v = 2[\mathrm{m/s}]$, sampling time $h = 1[\mathrm{s}]$. Sensor and pollution source parameters are set to the ones presented in Fig. 1.

Although increasing the dimension of the decision variables results in an slightly better information towards the end of the motion, but the solution with constant heading has more information during the initial phase of the motion. This is due to the fact that the ASV avoids going straight towards the source, which otherwise results in a singular FIM thereby making the system unobservable [14]. In general, piecewise constant course angles would be useful if the source location is known a-priori to some extent. But in the context of source seeking where the source location is unknown a priori, constant course angle would be a better strategy. Notice also that any chosen course angle needs to be revised as we get more measurements and update the information about source location. Thus, a good strategy should increase information in short and long term.

Case II (with current): In this case, the pollutant particles are advected by constant current vector. However, the analysis is similar to that of the previous case but in this case the optimal course angle will depend on the current vector. Contrary to the previous case, in this case there is a global

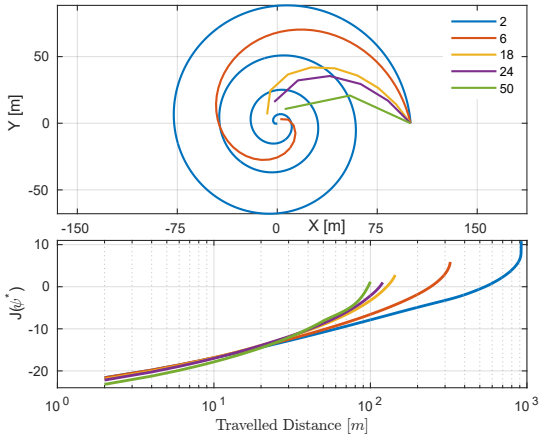

Fig. 6: Source seeking result and corresponding evolution of FIM for different number of samples m.

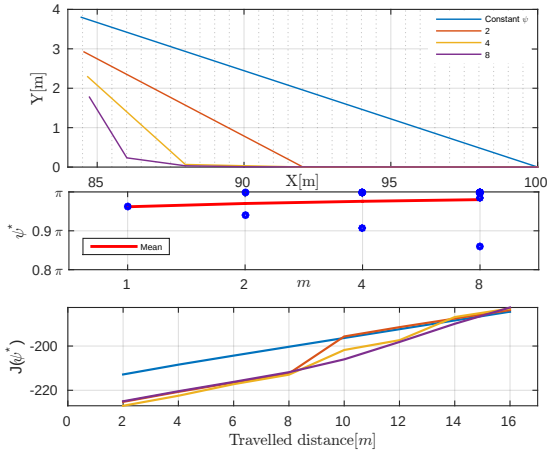

Fig. 7: Piecewise constant versus constant ψ planning ($m = 1$), for the case $\boldsymbol{v}_c = \mathbf{0}$: (top) resulting trajectory, (middle) derived $\boldsymbol{\psi}^*$ shown by blue dots and its mean shown by red line, and (bottom) resulting cost function versus travelled distance.

maximum and a local maximum (see Fig. 4). As a result of maximizing information, the optimization problem finds the solution that brings the ASV towards the main stream of pollutant particles advected by the current vector. Thus, explaining the global maximum solution. Except for the case that the current vector is aligned with relative position vector of the ASV with respect to the source, where both maximizers would result in the same FIM.

Next, consider the multi-variable cost function (6). Similar to the case without current, the resulting cost function has two maxima where one lies in $(\pi/2, \pi]^{m-1}$ and the other in $[-\pi, -\pi/2)^{m-1}$, with the difference that one is local and the other global maximum. Fig. 8 presents the multi-variable optimization results for different values of m, ASV speed $v = 2[\mathrm{m/s}]$, sampling time $h = 1[\mathrm{s}]$. Sensor and pollution source parameters are set to the ones presented in Fig. 1. The resulting solutions are so close to each other that there is no need to go for a piecewise constant course angle and constant course angle strategy would suffice. It is worth mentioning that in cases where angle of current vector is close to 0 or

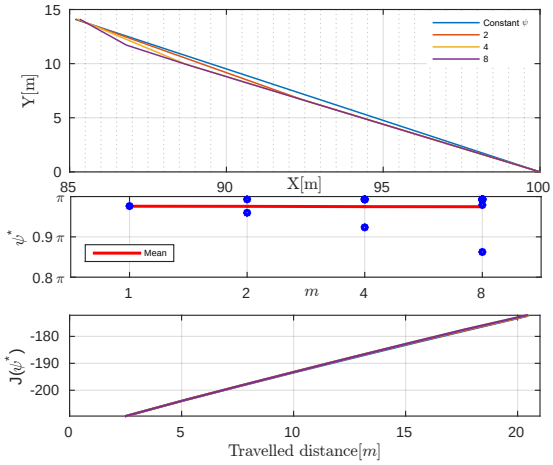

Fig. 8: Piecewise constant versus constant ψ planning ($m = 1$), for the case $\boldsymbol{v}_c = [0, 1]'$: (top) resulting trajectory, (middle) derived $\boldsymbol{\psi}^*$ shown by blue dots and its mean shown by red line, and (bottom) resulting cost function versus travelled distance.

π, there is a slightly more information gain for a piecewise constant course angle. But, due to the same reasoning as in the case of no current, we would consider a constant course angle strategy.

So far our emphasis was on investigation of optimal trajectories for maximizing information about a pollutant source location under the assumption that estimates are available. In the next subsection we focus on the estimation of the source location using the measurements.

B. Monte Carlo Pollutant Source Localization

In this part, we use the Monte Carlo method, also known as the PF [15], for the estimation of the pollutant source location. Since the ASV position is known through GPS measurements, the estimated pollutant source location may in turn be updated once the ASV measures the pollutant level at different locations. The Monte Carlo process has two steps: i) prediction update and ii) measurement update. The PF starts with multiple particles and each particle evolves according to the state equation. The re-sampling of the particles is performed so as to make the distribution of particles consistent with the measurements.

Multiple particles contain information about the pollutant source location $\boldsymbol{s}$ and the source emission rate Q_0. For each particle, the predicted pollutant measurement at a given ASV location is calculated using the estimated relative distance between the ASV location and the estimated source location of the particle, current velocity vector, and the nonlinear emission rate (1). During the measurement update, the actual pollutant measurement is used for importance sampling (see [16]) to update the weights of all particles. The accuracy of the estimate improves over time due to the inclusion of new measurements taken by the ASV.

In this section the subscript and superscript represent the time instant and the particle index, respectively, while over-bar denotes the predicted value. In the sequel $N > 0$ denotes the number of hypotheses.

1) Description of the PF for Pollutant Source Localization: Particles represent multiple hypotheses for $\boldsymbol{s}$ and Q_0 at time t denoted by $\boldsymbol{x}_t^{(k)} \triangleq [\boldsymbol{s}_t^{(k)}, Q_{0,t}^{(k)}]'$, $k \in \{1, 2, \dots N\}$. The prediction update $\bar{\boldsymbol{x}}_t^{(k)}$ of the kth hypothesis, $k \in \{1, \dots, N\}$, at time t is realized through the estimated relative distance constraint imposed by the present ASV location and the pollutant source location.

For each $k \in \{1, \dots, N\}$, compute the predicted relative distance $\bar{q}_t^{(k)} = \|\boldsymbol{r}_t - \bar{\boldsymbol{s}}_t^{(k)}\|$ and the predicted pollutant emission rate $\bar{R}_t^{(k)}$ using (1). Using these information, then compute the predicted mean concentration $\bar{\mu}_t^{(k)} = \bar{R}_t^{(k)}(\boldsymbol{r}_t, \bar{\boldsymbol{s}}_t^{(k)})\Delta t$. The probability that the sensor at location $\boldsymbol{r}_t$ encounters z pollutant particles is then calculated using the predicted mean concentration $\bar{\mu}_t^{(k)}$ as described in (3). The measurement update is realized using the actual pollutant measurement z_t at time t. The pollutant source location $\boldsymbol{s}$ is estimated using the mean of multiple hypotheses of the estimated pollutant source location $\bar{\boldsymbol{s}}_t^{(k)}$.

2) Algorithm: Algorithm 1 summarizes the particle filter. Step 4 performs sampling which is equivalent to the *prediction update*. The sign $\sim$ in this step shows that $\boldsymbol{x}_t^{(k)}$ is sampled according to the distribution $p(\boldsymbol{x}_t^{(k)}|\boldsymbol{x}_{t-1}^{(k)})$. In this case, we assume the pollutant source is static. In step 4, (1) and (3) are used to predict the pollutant measurement at the present ASV location $\boldsymbol{r}_t$. Step 5 updates weights based on the pollutant measurement at ASV location $\boldsymbol{r}_t$. In step 6, the updated particles are added to the particle set of the posterior, while in step 8 the weights are normalized. If the dispersion of the importance weights, N_{eff}, is less than $N/2$, then resampling proportional to the weights of the particles is performed (step 11). Function $\text{resample}(\cdot)$ does this operation.

Algorithm 1 Particle filter for pollutant source localization.

Require: Set of particles representing pollutant source location $\boldsymbol{s}$ and emission rate Q_0 prior at time t: P_{t-1},
ASV location at time t: $\boldsymbol{r}_t$,
observation of pollutant at ASV present location at time t: z_t.

Ensure: Set of particles representing pollutant source location $\boldsymbol{s}$ and emission rate Q_0 posterior at time t: P_t.

1: $\text{P}_t \leftarrow \emptyset$
2: **for** $k = 1 \rightarrow N$ **do**
3: $\quad < x_{t-1}^{(k)}, w_{t-1}^{(k)} > \leftarrow \text{P}_{t-1}^{(k)}$
4: $\quad$ sample $x_t^{(k)} \sim p(x_t^{(k)}|x_{t-1}^{(k)})$ and obtain $\|\bar{\boldsymbol{s}}_t^{(k)} - \boldsymbol{r}_t\|$, $\bar{R}_t^{(k)}$ and $\bar{\mu}_t^{(k)}$.
5: $\quad \tilde{w}_t^{(k)} \leftarrow p(z_t|x_t^{(k)}, \boldsymbol{r}_t)\, w_{t-1}^{(k)}$
6: $\quad \text{P}_t \leftarrow \text{P}_t \cup < x_t^{(k)}, w_t^{(k)} >$
7: **end for**
8: $w_t^{(k)} \leftarrow \tilde{w}_t^{(k)} / \sum_{k=1}^{N} \tilde{w}_t^{(k)}$
9: **if** $N_{\text{eff}} < \frac{N}{2}$ **then**
10: $\quad$ **for** $k = 1 \rightarrow N$ **do**
11: $\quad\quad \text{resample}(\text{P}_t)$
12: $\quad$ **end for**
13: **end if**
14: return P_t

IV. Simulation Results

The performance of the source seeking algorithm is assessed through numerical simulations. In the simulated setup, the ASV moves with a magnitude of velocity $v = 2$, and the parameters of the sensor and diffusion process model are set to $a = 1$, $\tau = 250$, $Q_0 = 1$, $h = 1$, $\Delta t = 1$, and $D = 1$. Furthermore, look ahead horizon for the optimal control action is set to $m = 3$ samples.

We consider $N = 10,000$ number of uniformly spread random hypotheses in the search area of $[-15, 15] \times [-15, 15][\text{m}^2]$ for the PF and N random source emission rate $Q_0^{(k)}$ of the hypotheses are set according to a log-normal probability density function (PDF) with mean value of $\mu = 1$ and standard deviation of $\sigma = 1.2$.

Search algorithm is stopped when the area under the estimated PDF of source location within $\pm 2[\text{m}]$ radius is above 0.95, there by meaning that, ASV has more than 95% certainty that the source location is within $2[m]$ of the estimated location. The source seeking is terminated, if the algorithm fails to localize the pollutant source location within $500[\text{s}]$. Further, if the estimated source location is out of desired bound ($\pm 2[\text{m}]/\pm 5[\text{m}]$), it is considered as false localization.

We demonstrate two scenarios for evaluation of the proposed algorithm through simulations. In the first scenario, the behavior of the source seeking algorithm is illustrated for one specific case. The results are shown in Fig. 9 and discussed. In the second scenario, we run the algorithm for $n = 1000$ trials with random initial conditions to check the consistency of source seeking method. In the following, each scenario is described in more details.

A. Illustrative Scenario

In this scenario, initial location of the ASV is at $\boldsymbol{r}_0 = [10, -15]'$, the pollutant source is located at $\boldsymbol{s} = [-10, 3]'$, and the current velocity vector is set to $\boldsymbol{v}_c = [1, 0]'$.

Fig. 9 shows numerical results of the illustrative scenario where black markers represent detected pollutants at sampling locations and size of the markers are proportional to number of pollutant particles detected. Green dots denote multiple hypotheses (particles of PF) of pollutant source location. The column shows initial distribution of hypotheses for $\boldsymbol{s}$ and Q_0, and the right column depicts the final distribution after termination of source seeking algorithm.

The ASV starts the mission by going up and slightly towards the center of search area. As it detects pollutant particles in the main stream of the pollutant source, it moves towards the source in a shrinking zig-zag maneuver and interestingly this trajectory has a close similarity to the trajectories followed by flying moths as reported in [17][1]. It passes the source location ($\pm 1[\text{m}]$) after $64[\text{s}]$ of the start of the mission and after traveling $97.8[\text{m}]$ but due to low certainty about the source location (84.2%) it moves

[1]Thanks to the anonymous reviewer for bringing this into our notice.

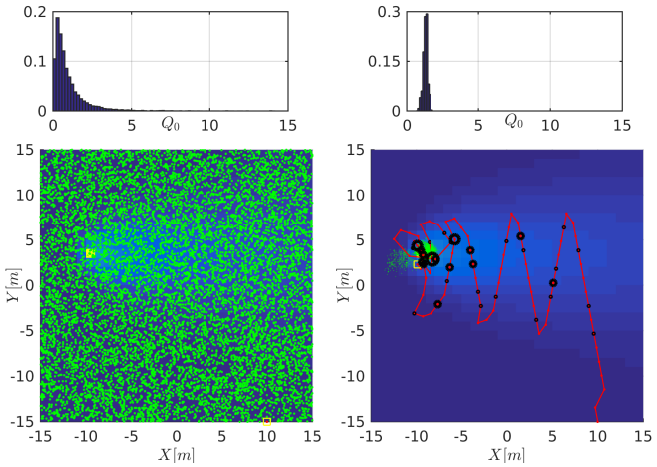

Fig. 9: Numerical results of the illustrative scenario, where black markers represent detected pollutants, (left) initial distribution of hypotheses, and (right) final distribution after termination of source seeking.

around the source until the seeking terminates at 84[s], after 129.3[m] of traveling distance, with probability 97%, and final source location estimation error 1.34[m].

B. Random Scenario

In this case consistency of the proposed seeking method is evaluated by running $n = 1000$ random scenarios. Initial location of the ASV is set to a random location on the boundary of the search area. Pollutant source location is at a random location in the area of $[-10, 10] \times [-10, 10][\mathrm{m}^2]$. Moreover, direction of the current is picked from a uniform distribution in $[0, 2\pi]$. In average, each run took 7.43[s] ($\sigma = 1.67$[s]) of computation time on an Intel Core i7-4770 CPU with 16GB of RAM for an average mission time of 62.2[s] ($\sigma = 24.4$[s]). Various statistical metrics are tabulated in Table I and they are comparable with illustrative scenario.

Metric	Value
Fail rate	1.2%
False localization rate ± 2[m]	9.3%
Successful localization rate ± 2[m]	89.5%
False localization rate ± 5[m]	1.2%
Successful localization rate ± 5[m]	97.6%
Average localization error $E[\bar{\boldsymbol{s}} - \boldsymbol{s}]$	$[0.47, 0.5]'$[m]
Covariance of localization error $Cov[\bar{\boldsymbol{s}} - \boldsymbol{s}]$	$\begin{bmatrix} 1.07 & -0.09 \\ -0.09 & 1.29 \end{bmatrix}[\mathrm{m}^2]$
Normalized traveled distance $(\mu, [\sigma])$	$6.03[2.90]$
Traveled distance $(\mu, [\sigma])$	$101.9[38.9]$[m]
Mission time $(\mu, [\sigma])$	$62.2[24.4]$[s]
Computation time $(\mu, [\sigma])$	$7.43[1.67]$[s]

TABLE I: Statistical results of $n = 1000$ random initial condition runs of the proposed source seeking algorithm

V. Conclusions and Future Directions

Motivated by applications, in this paper we proposed a optimal motion planning for an ASV carrying a pollutant sensor for source seeking, where the emphasize is to maximize pollutant related measurement information available for the source localization. We use an appropriately defined Fisher information along the trajectory of the ASV that is computed on a moving-horizon interval of decision, which allows to incorporate the new information available for optimal motion planning. Future work includes the implementation of the proposed method on the environmental monitoring robot (Envirobot [8]) to collect real-world data and test it in an experimental setup. Further, exploring optimal actions for $m = 3$ to find a solution that is most compatible with the locomotion of Envirobot. Interestingly, the Envirobot locomotion is combination of a straight line forward motion while exciting lateral movements. Finally, another direction of future research is to extend the proposed framework to 3D source seeking considering a similar extended 3D model of the diffusion process.

References

[1] R. A. Russell, A. Bab-Hadiashar, R. L. Shepherd, and G. G. Wallace, "A comparison of reactive robot chemotaxis algorithms," *Robotics and Autonomous Systems*, vol. 45, no. 2, pp. 83–97, 2003.

[2] L. Paull, M. Seto, and H. Li, "Area coverage planning that accounts for pose uncertainty with an AUV seabed surveying application," in *IEEE International Conference on Robotics and Automation (ICRA)*. IEEE, 2014, pp. 6592–6599.

[3] G. Ferri, M. V. Jakuba, A. Mondini, V. Mattoli, B. Mazzolai, D. R. Yoerger, and P. Dario, "Mapping multiple gas/odor sources in an uncontrolled indoor environment using a Bayesian occupancy grid mapping based method," *Robotics and Autonomous Systems*, vol. 59, no. 11, pp. 988–1000, 2011.

[4] W. Li, J. A. Farrell, S. Pang, and R. M. Arrieta, "Moth-inspired chemical plume tracing on an autonomous underwater vehicle," *IEEE Transactions on Robotics*, vol. 22, no. 2, pp. 292–307, 2006.

[5] L. Champagne, R. G. Carl, and R. Hill, "Agent models II: search theory, agent-based simulation, and U-boats in the Bay of Biscay," in *Proceedings of the 35th conference on Winter simulation: driving innovation*. Winter Simulation Conference, 2003, pp. 991–998.

[6] M. Vergassola, E. Villermaux, and B. I. Shraiman, "Infotaxis as a strategy for searching without gradients," *Nature*, vol. 445, no. 7126, pp. 406–409, January 2007.

[7] B. Ristic, A. Skvortsov, and A. Gunatilaka, "A study of cognitive strategies for an autonomous search," *Information Fusion*, vol. 28, pp. 1–9, March 2016.

[8] Envirobot Project. (2013-2017). [Online]. Available: http://wp.unil.ch/envirobot/

[9] D. Moreno-Salinas, N. Crasta, M. Ribeiro, B. Bayat, A. M. Pascoal, and J. Aranda, "Integrated motion planning, control, and estimation for range-based marine vehicle positioning and target localization," in *IFAC Conference on Control Applications in Marine Systems (CAMS)*, Trondheim, Norway, September 2016.

[10] N. M. Temme, *Special functions: An introduction to the classical functions of mathematical physics*. John Wiley & Sons, 2011.

[11] Y. Bar-Shalom, X. R. Li, and T. Kirubarajan, *Estimation with applications to tracking and navigation: Theory algorithms and software*. John Wiley & Sons, 2001.

[12] M. Bayat, N. Crasta, A. P. Aguiar, and A. M. Pascoal, "Range-based underwater vehicle localization in the presence of unknown ocean currents: Theory and experiments," *IEEE Transactions on Control Systems Technology*, vol. 24, no. 1, pp. 122–139, January 2016.

[13] M. Pedro, D. Moreno-Salinas, N. Crasta, and A. Pascoal, "Underwater single-beacon localization: Optimal trajectory planning and minimum-energy estimation," in *IFAC Workshop on Navigation, Guidance and Control of Underwater Vehicles (NGCUV)*, Girona, Spain, April 2015.

[14] C. Jauffret, "Observability and Fisher information matrix in nonlinear regression," *IEEE Transactions on Aerospace and Electronic Systems*, vol. 43, no. 2, pp. 756–759, 2007.

[15] D. Simon, *Optimal state estimation: Kalman, H-infinity, and nonlinear approaches*. John Wiley & Sons, 2006.

[16] B. Ristic, S. Arulampalam, and N. Gordon, *Beyond the Kalman filter: Particle filters for tracking applications*. Artech House, 2004.

[17] A. Mafra-Neto and R. T. Cardé, "Fine-scale structure of pheromone plumes modulates upwind orientation of flying moths," *Nature*, vol. 369, pp. 142–144, 1994.